TENSILE FAILURE PREDICTION AND MEASUREMENT IN COMPOSITE SCARF REPAIR

Iarve, Endel V.*, Breitzman, Timothy D., Cook, Benjamin M.** ,**
Schoeppner, Gregory A., Mollenhauer, David H.****
***University of Dayton Research Institute, Dayton OH,**
****Air Force Research Laboratory, WPAFB OH**

Keywords: *Composite, Scarf Repair, Strength, Fiber Failure, Interfacial Strength*

Abstract

Oversized quasi-isotropic tensile specimens were manufactured from IM6/3501-6 graphite/epoxy prepreg. Seven specimens were scarfed in the center of the panel, and four of the panels were subsequently repaired. The repair patch consisted of a ply-by-ply replacement of the removed material with a FM-300M-05 film adhesive placed between the repair patch and the scarfed specimen. The patch and adhesive were then co-cured. The repaired and unrepaired specimens were strain gaged and tested to failure. A three-dimensional failure analysis was performed. The strength prediction was based on the state of stress in the 0° plies by taking into account the redistribution of stress due to adhesive failure. The performed analysis accurately predicted both the strength of the scarfed and repaired panels based solely on properties characterized by testing unnotched standard coupons.

1 Introduction

The use of flush or nearly flush repairs for composite structures to maintain strict aerodynamic outer mold line requirements is a technology that is increasingly becoming essential to maintaining composite-dominated aircraft structures. Unfortunately, there are only a limited number of studies on scarf repairs and patches. The published studies have described both experimental and numerical/analytical evaluation of the strains and failure loads of tension and compression loaded test articles and some of the shortcomings of current capabilities (for example [1,2]).

2 Specimen Preparation and Testing

Panels measuring 30 cm × 61 cm (12 in × 24 in) with a $[45/0/-45/90]_S$ stacking sequence were manufactured using IM6/3501-6 graphite/epoxy unidirectional prepreg. The panels were trimmed and cut in half to yield 13.31 cm × 57.15 cm (5.25 in × 22.5 in) test specimens. Scarfing of the specimens was accomplished with the apparatus shown in Figure 1. The apparatus uses a diamond bit with a pneumatic grinder that is rotated around a 2.54cm (1.0in) center hole and translated to provide a repeatable scarf cutout. A 20:1 scarf angle was maintained for the specimens. Additionally, the apparatus was used to cut out the scarf patches from laminates identical to those of the parent specimens.

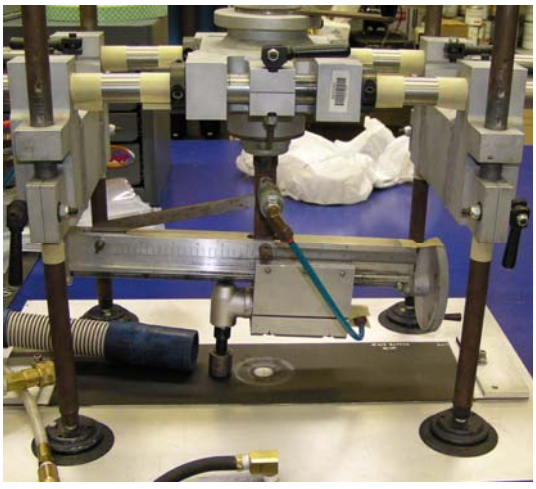

Figure 1. Scarfing apparatus

The scarf patches were bonded to the parent specimens using Cytec Fiberite's FM-300M-05 adhesive cured according to manufacturers instructions. Additionally, a single over-ply

extending onto the parent specimen was added to the top of the scarf patch to help in load transfer between the patch and parent specimen. The adhesive as well as the over-ply were cured using a 176ºC (350ºF) cure cycle. The specimens were instrumented with uniaxial and rosette strain gages to monitor the far- field surface strains, the strains on the patch over-ply, and strains adjacent to the patch on the parent specimen during tensile loading of the specimens. At various plane view locations on the specimen, back-to-back (front and back of the specimen) gages were mounted to measure localized bending strains caused by eccentricity of the specimen response. Glass reinforced epoxy tabs were bonded to the specimens with EPON 828 epoxy, a room temperature cure bonding system with EPI-CURE 3140 as the hardener. The tensile load was introduced into the specimens in the tab region through bolted fixtures. In addition, 10 standard tensile specimens of in-plane dimension 25.4cm by 2.54cm (10 by 1 in) were tested for obtaining fiber direction strength properties. More details regarding specimen preparation can be found in reference [3].

3 Strength Prediction

Spline approximation based 3D ply level analysis was used for failure prediction. The plate, adhesive and the repair patch models are shown on Figure 2.

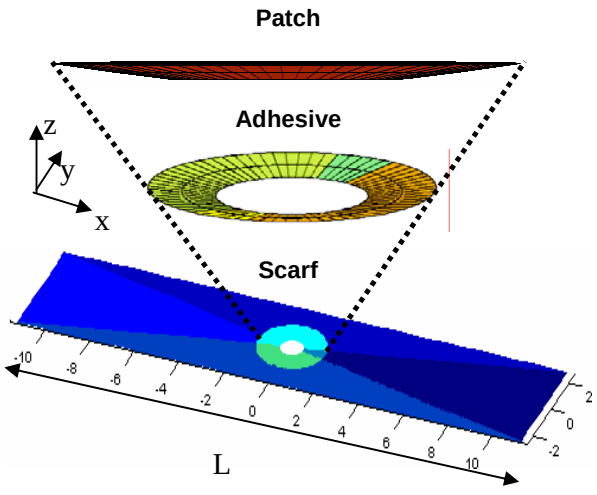

Figure 2. Computational model for the scarfed plate, patch and adhesive.

A layer of cohesive interface elements between the scarf and adhesive was utilized to model the delamination of the adhesive from the parent specimen as a function of load. At the same time the fiber failure in the scarfed panel was predicted by using the critical failure volume (CFV) method recently proposed in [4]. The average applied load for fiber failure was predicted at each load level characterized by a state of delamination in the adhesive/scarfed panel interface. Initially, the stress distribution in the repaired panel is homogeneous and the fiber failure stress predicted is identical to that of virgin laminate. The increase of the applied load leads to initiation and growth of the delamination between the repair patch and the plate. The stress distribution in the patch becomes nonuniform with the stress concentration typical of open hole composites. At some applied load the average predicted fiber failure load and the applied load become equal. This load value is considered the failure load for the repaired panel.

4 Critical Failure Volume Method

The fiber failure load in the scarfed panel was predicted by using the CFV method [4]. The critical failure region in a quasi-brittle material under nonuniform stress state is defined as a finite subvolume, which has the highest probability of complete loss of load carrying capacity. An algorithm is proposed to find such a volume, which does not involve a concept of subdivision into mesh cells but instead deals with parametric representation of the nonuniform stress fields. The probability of failure or loss of load carrying capacity in the case of uniform stress field is considered to follow a Weibull distribution

$$f(\sigma,V) = 1 - e^{\frac{V}{V_0}B(\sigma)} \qquad (1)$$

The assumption, which we will use to evaluate the probability of failure in the nonuniformly loaded regions, states that eqn. (1) provides a lower bound of probability of failure of a specimen with nonuniform stress distribution, if the stress in each point is higher or equal to σ. Thus the probability of failure P of a nonuniformly stressed specimen with stress distribution $\sigma(\mathbf{x})$ can be estimated as

$$P \geq f(\sigma_u, V), \qquad (2)$$

if

$$\sigma_u = \min_{\mathbf{x}\in V}(\sigma(\mathbf{x})). \quad (3)$$

The estimate given by eqn. (2) is not very useful when applied to the entire volume of the specimen. On the other hand, one can select a finite region in the nonuniformly loaded specimen, which has a volume V_i and minimum stress of σ_i, and calculate the probability of failure for this subvolume $f(\sigma_i,V_i)$. Suppose that we have found a subregion with volume V_c and minimum stress σ_c, for which this probability is the highest, i.e.

$$f(\sigma_c, V_c) = \max_i f(\sigma_i, V_i), \quad (4)$$

where index *i* scans all subregions of the specimen. Then the subregion V_c will have the highest probability of local failure, and we will call it critical failure volume (CFV).

We shall now describe an algorithm for identification of the CFV and calculation of its failure probability f_{CFV}. Denote the magnitude of the maximum stress as σ_m. Introduce a set of iso-stress surfaces $q_i\sigma_m$, $q_0=1>q_1>q_2>q_3\ldots>0$. Consider a continuous function $v(q)$, $0 \le q \le 1$:

$$v(q) = \mathrm{vol}(V_q), \{\mathbf{x} \in V_q \Leftrightarrow \sigma(\mathbf{x}) \ge q\sigma_m\} \quad (5)$$

This function is equal to the volume of the specimen with stress higher or equal to $q\sigma_m$. The lower bound of the probability of failure for these volumes can be estimated as $f(q\sigma_m, v(q))$ by using Eqn.(1). The latter is a continuous function and its local maximum (if it exists) corresponds to the probability of failure of CFV

$$f_{CFV} = \max_q f(q\sigma_m, v(q)). \quad (6)$$

Denote by q_c the value of q for which $f_{CFV}=f(q_c\sigma_m, v(q_c))$ then the respective stress contour $q_c\sigma_m$ bounds the CFV and its volume will be equal to

$$V_c = v(q_c). \quad (7)$$

The existence of a meaningful value $0<q_c<1$ depends upon both the stress field characteristics as well as that of the material. In the present paper, we will limit ourselves to finite values of σ_m. For an arbitrary stress distribution, which defines the volume function v(q), this function can have complex shape. For a typical open hole problem and shape function $B(\sigma)$ in the form of a two parameter distribution

$$B(\sigma) = \left(\frac{\sigma}{\beta}\right)^{\alpha}, \quad (8)$$

where α – is the Weibull modulus or shape parameter and β is an additional constant, one obtains $f=0$ for $q=0$ and $q=1$. This means that the function $f(q\sigma_m, v(q))$ will have at least one local maximum $(f \ge 0)$ for $0<q<1$. The fact that $f=0$ for $q=1$ follows from the premise that the maximum stress is attained at a point associated with zero volume, i.e. $v(1)=0$.

5 Physics based limits of CFV

At the root of the CFV method is identification of the most likely failure region by finding the value q_c and tracing the region bounded by the stress value of $q_c\sigma_m$ and/or evaluating its volume V_c. As shown in Ref. [4] this capability becomes essential in predicting the fiber failure in composite laminates with stress concentrations. In particular, it was shown that the linear size of CFV defined as

$$l_c = \sqrt{V_c / h},$$

where *h* is the thickness of the ply, estimated for quasi-isotropic T300/934 laminates with small 2.54mm diameter holes, was significantly below the value of the ineffective length δ introduced by Rosen [6]. It is clear that the strength scaling parameters in Eqn. (8), which are obtained by testing laboratory size specimens are not valid when $l_c \sim \delta$. Thus the probability of failure f_{CFV} becomes meaningless if V_c (l_c) is too small. Suppose that one has an estimate of the minimum size volume V_{min} for which the Weibull scaling in the form (1) and (8) is valid. In the case of fiber failure, such limits were investigated in Ref. [7] by performing Monte-Carlo simulation of failure of square cross sections of fiber bundles of three different length 3δ, 6δ and 9δ. A value of $l_{min}=6\delta$ was considered the minimum scalable length in their study for fibers with Weibull modulus in the range of 10. Although this is higher

then the values of 5-6 for typical carbon fibers it can be used to estimate V_{min} as

$$V_{min}= l_{min}^2 h\,. \tag{9}$$

Having a value of V_{min} one can *apriori* evaluate the validity of a f_{CFV} prediction comparing V_c and V_{min}. However, more importantly if $V_c<V_{min}$ and the value of f_{CFV} is physically inadmissible, one can simply obtain another physically admissible estimate of the probability of failure by finding the maximum local probability of failure of only those subvolumes which are larger or equal to V_{min}. In other words we will replace the definition of CFV given by Eqn. (6) by slightly modified one

$$f_{CFV} = \max_{\substack{q \\ v(q)\geq V_{min}}} f(q\sigma_m, v(q)). \tag{10}$$

The practical calculation of a new value of q, say q_0, such that $f_{CFV}=f(q_0\sigma_m, v(q_0))$ satisfies Eqn. (10) is also straight forward at least in the case when V_{min} and V_c are both much smaller then the specimen volume. In this case q_0 is simply calculated by solving the equation $v(q_0)=V_{min}$. Indeed if q_c provides an absolute maximum for the function $f(q\sigma_m, v(q))$ then the conditional maximum, such that $v(q) \geq V_{min}$ will take place at $q=q_0$ as long as the function $f(q\sigma_m, v(q))$ is monotonic on the interval $q_0 \leq q \leq q_c$.

It might appear that the correction for the minimum scalable volume is an issue pertaining to the CFV method. On the contrary, this is a problem related to material heterogeneity and stress concentration in any volumes in which size becomes comparable to the scale of the microstructure. It will be shown below that the Weibull integral calculated in problems when the application of the CFV method shows $V_c<V_{min}$ gives unacceptably conservative strength values due to the fact that most of the contribution to the Weibull integral comes from the very region V_c. However, due to its integral nature there are no simple modifications to solve this problem. The solution proposed by Bazant in the 90's and known as nonlocal Weibull theory [8] proposes to first calculate stress averages over certain physically dictated characteristic volumes such as V_{min} and then use these averages in the secondary integration of the Weibull integral. Such approach clearly addresses the problem at hand, but requires considerably more effort for practical implementation.

6 3D Stress Analysis and v(q) function calculation

Consider a rectangular orthotropic plate containing a throughout circular scarfed hole having a smaller diameter d at z=0 and larger diameter D at z=H, as shown in Figure 2. The plate consists of N plies of total thickness H in the z-direction and has a length L in the x-direction and width A in the y-direction. The following displacement boundary conditions were applied to the specimen

$$u_x(0, y, z) = u_y(0,0,0) = u_z(x, y,0) = 0 \tag{11}$$

Traction boundary condition was applied at the x=L end, so that

$$\sigma_{xx}(L, y, z) = T$$

All other surfaces were traction free. Such mixed traction/displacement formulation was utilized to combine the mechanical and thermal loading, which was used to account for the effect of residual stress. The constitutive relations of each ply are as follows:

$$\sigma_{ij} = C^p_{ijkl}(\varepsilon_{kl} - \alpha^p_{kl}\Delta T)\,,\ \text{i=1,…,N,}$$

where C^p_{ijkl} and α^p_{kl} are elastic moduli and thermal expansion coefficients of the p^{th} orthotropic ply, and ΔT is the temperature change. The average applied traction was then calculated as

$$\sigma_0 = \int_{y,z} \sigma_{xx}(0, y, z)dydz \tag{12}$$

where x_c , y_c are the coordinates of the center of the hole.

A three-dimensional ply level stress analysis in realistic composite laminates containing holes represents a formidable problem if using a standard finite element programs. A B-spline displacement approximation approach developed by Iarve [9] was shown to provide highly accurate stress solutions in the immediate vicinities of the ply interface and hole edge intersections, where there is singular stress behavior.

The three-dimensional approximation is built by using the tensor product of one-dimensional approximations. Consider an elementary cube $[0,1]^3$ in local x_1, x_2, x_3 coordinate system, then the 3-D displacement approximation can be written as

$$\mathbf{u}(x_1 x_2 x_3) = \sum_i \sum_j \sum_k X_i(x_1) Y_j(x_2) Z_k(x_3) \mathbf{U}_{ijk} \quad (13)$$

where u is the displacement vector and $U_{i,j,k}$ are vectors of displacement approximation coefficients not necessarily associated with nodal displacements, and indeces *i*,*j* and *k* in equation (13) change from 1 to the total number of approximation functions in each direction. Depending upon the application and geometry, different orders of splines (from 1 to 8) can be used in each direction. Besides changing the order of splines, one can also change their defect (maximum number of discontinuous derivatives) in the node, thus being able to apply standard linear or a higher order p-type finite element approximation if desired. Curvilinear coordinate transformation $x=x(x_1\ x_2\ x_3)$, $x^T=(x,y,z)$ with Jacobian matrix J $(x_1\ x_2\ x_3)$ is used to map the unit volume into the global x,y,z, coordinate system. The Gaussian integration procedure is used to calculate the components of the stiffness matrix. For purposes of the present study, we shall describe the procedure of calculating the overstressed volume function v(q). After the solution is completed and all vectors $U_{i,j,k}$ are determined, a post-processing step is performed when each integration point of the structure is examined twice. First the stress and strain components are computed, and the maximum value σ_m of the component of interest is found by searching through all integration points. A large number M (in our analysis M=101 and 201) is then prescribed, and a sequence

$q_i = 1-i/M$, i=0,…,M,

defined. The overstressed volume function v(q) is then calculated in M points as

$$v(q_i) = \sum_{g_1} \sum_{g_2} \sum_{g_3} w_{g_1} w_{g_2} w_{g_3} \det J(x_1^{g_1}, x_2^{g_2}, x_3^{g_3}) \times \eta(\sigma - q_i \sigma_m) \quad (14)$$

by using the Heaviside step function

$$\eta(\sigma) = \begin{cases} 1, \sigma > 0 \\ 0, \sigma \le 0 \end{cases} \quad (15)$$

In equation (14) indexes g_i, *i=1,2,3* denote Gauss integration points in x_1 x_2 and x_3 directions, respectively, and w_{gi} are respective Gaussian weights. Step function (15) cuts off the contribution from all integration points where the stress is lower than the threshold $q_i\sigma_m$. For low values of the threshold value, v(q) will include almost all integration points in (14) and become close to the entire volume. The probability f_c is then calculated according to equations (10).

7 Results and Discussion

The unidirectional properties of the IM6/3501-6 material were as follows: E_{11}=175.27Gpa, $E_{22}=E_{33}$=9.79Gpa, $v_{13}=v_{13}$=0.33, v_{23}=0.49, $G_{12}=G_{13}$=5.51Gpa and G_{23}=2.96Gpa, with the coefficient of thermal expansion of $\alpha_{11}=4.10^{-6}C^0$ and $\alpha_{22}=32\ 10^{-6}C^0$ The Weibull parameters for the strength in the fiber direction were equal to X_t=2.06Gpa, V_0=1638.7mm^3 and Weibull modulus α=40. The value of the Weibull modulus was taken from Wisnom et al. [5]. The l_{min} =0.266mm was calculated according to reference [4]. The initial elastic properties of the adhesive were E=3.1Gpa, v=0.38 and the thermal expansion coefficient was $\alpha=0.62\cdot10^{-6}C^0$. The ply and adhesive thickness were h=0.13mm. The temperature change $\Delta T=-155^0C$. At low loads prior to the delamination on the adhesive/panel interface, the stress field in the scarfed panel is quite uniform, as shown on the Figure 3. No stress concentration typical of an open hole is present. The average fiber failure load is predicted equal to that of virgin panels.

In the case of scarfed open hole panels a severe stress concentration typical of an open hole exists, Figure 4.a. The strength of such panels is about 1/3 of the virgin panels and is predicted accurately by using the CFV method. The experimental and theoretical results are shown on Figure 5. In the case of repaired panels the stress concentration at 90% of the failure load is shown on Figure 4.b. The stress

(a)

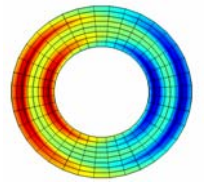

(b)

Figure 3. Normal σ_{xx} stress distribution in the adhesive (a) and the scarfed plate prior to any delamination on the adhesive/panel interface

concentration is less severe than in the case of open scarfed hole and the predicted strength values of the repaired panels are at the level of 2/3 of the intial virgin panel strength.

(a)

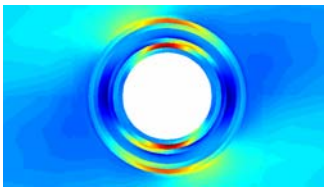

(b)

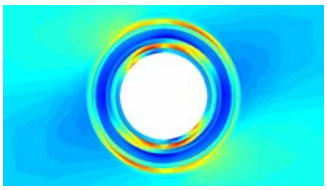

Figure 4. Normal σ_{xx} stress distribution in the scarfed and repaired panels. Open scarfed hole (a) and partially delaminated adhesive at 90% of the scarf failure load (b).

Experimental data and predicted strength values for small and large size unnotched tensile coupons, as well as strength of scarfed open hole and scarfed repaired panels are shown on Figure 5. Significant reduction in experimentally measured strength of large virgin panels as compared to small coupons as well as only 5% predicted reduction due to volume increase is attributed to grip failure of most large virgin specimens. However, the unrepaired and repaired scarfed laminates exhibited brittle failure through the cavity.

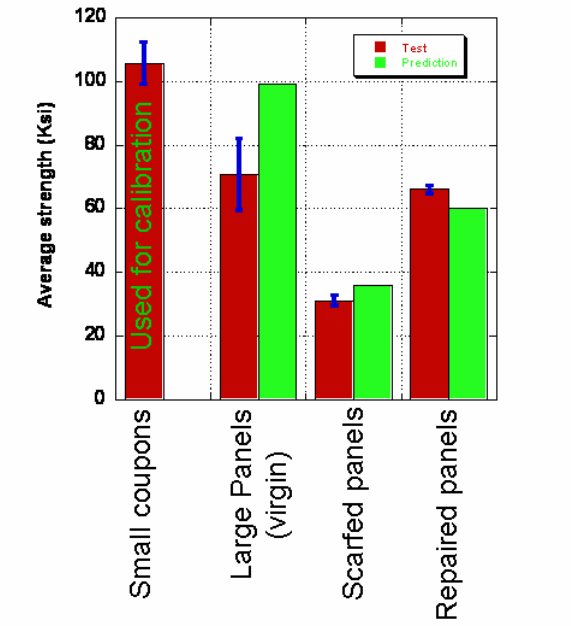

Figure 5. Experimental and numerical results

The strength of the repaired panels is strongly affected by the amount of failed adhesive. The predicted strength values for both cases are close to those measured experimentally and overall a good agreement is observed.

Acknowledgement

The first two authors are grateful for AFOSR support under grant FA9550-04-1-0142 and AFRL contract FA8650-05-D-5052.

References

[1]. Soutis, C. and F.Z. Hu. “A 3-D Failure Analysis of Scarf Patch Repaired CFRP Plates,” *American Institute of Aeronautics and Astronautics, Inc.*, Paper number AIAA-98-1943 pp. 1971-1977 (1998).

[2]. Found, M.S. and Friend, M.J., ”Evaluation of CFRP Panels with Scarf Repair Patches,”

Composite Structures, Vol. 32, pp. 115-122, (1995)

[3]. Cook, B.M, "Experimentation and Analysis of Composite Scarf Joint," M.S. Thesis, Air Force Institute of Technology, March 2005.

[4]. Iarve, E.V., R. Kim and D. Mollenhauer, (2007) "Three-dimensional Stress Analysis and Weibull Statistics Based Strength Prediction in Open Hole Composites", *Composites Part A*, **38**, pp 174-185

[5]. Wisnom, M. R., B. Khan, B. Green, W. Jiang and S. R. Hallet (2005), "Specimen Size Effects on Tensile Strength and Failure Mechanisms of Carbon/Epoxy Composites," *JNC14 Conference*, Compiegne, France, March 2005

[6]. Rosen, B.W. (1964) "Tensile Failure of Fibrous Composites," *AIAA Journal*, **2**, 1985-91

[7]. Landis, C. M., I. J. Beyerlin, & R. M. McMeeking. (2000). "Micromechanical Simulation of the Failure of Fiber Reinforced Composites." *Mechanics and Physics of Solids*, *48* (621-648).

[8]. Bazant, Z.P., (2002), "Scaling of Structural strength", Hermes Penton Science (Kogan Page Science), London

[9]. Iarve, E.V. (1996) "Spline Variational Three-Dimensional Stress Analysis of Laminated Composite Plates with Open Holes," *Int. J. Solids & Structures*, 44(14), pp. 2095-2118**.**